Multilayers with high-reflectivity at 19.5 nm and low-reflectivity at 30.4 nm

Li Jiang (蒋 励)[1], Jingtao Zhu (朱京涛)[1], Zhong Zhang (张 众)[1], Zhanshan Wang (王占山)[1*], Michael Trubetskov[2], and Alexander V. Tikhonravov[2]

[1] *Department Institute of Precision Optical Engineering, Department of Physics, Tongji University, Shanghai 200092, China*

[2] *Lomonosov Moscow State University, Russia*

[*] *Corresponding author: wangzs@tongji.edu.cn*

Received December 6, 2012; accepted December, 26 2012; posted online June 7, 2013

The multilayer (ML) mirror with high-reflectivity (HR) at a specific emission line of 19.5 nm (Fe line) and low-reflectivity (LR) at 30.4 nm (He line) is needed to be designed and fabricated for observing the image of sun. Based on a variety of optimizations utilized different structures, the design is performed and the final results demonstrate that the reflectivity at 30.4 nm does not achieve minimum value when the reflectivity at 19.5 nm reaches the maximum value. The tradeoff should be done between the HR at 19.5 nm and LR at 30.4 nm. One optimized mirror is fabricated by direct current magnetron sputtering and characterized by grazing-incident X-ray diffraction (XRD) and synchrotron radiation (SR). The experimental results demonstrate that the ML achieves the reflectivity of 33.3% at 19.5 nm and of 9.6×10^{-4} at 30.4 nm at the incident angle of 13°.

OCIS codes: 240.0310, 310.4165.

doi: 10.3788/COL201311.S10606.

The development in multilayer (ML) coatings with nanometer-scale periods operated as efficient mirrors in the extreme ultraviolet (EUV) has enabled the construction of instrumentation using normal-incidence ML optics for solar physics researches[1]. High resolution Cassegrain telescopes, such as SDO, TRACE, and SOHO/EIT[2−4], coated with narrow-band MLs worked at specific coronal or transition-region emission lines have achieved unprecedented success[5,6]. As we known, how to suppress the influence of He line II (30.4 nm) is a big challenge for observing Fe XII (19.5 nm) line because the former line is much stronger than other specific emission lines of sun. In order to find an efficient solution for the suppression of unwanted He II radiation, we design and deposite a new ML with high-reflectivity (HR) at 19.5 nm and low-reflectivity (LR) at 30.4 nm. The measured performance of this ML is shown in this letter.

In the EUV region, the near unity of the real part of the refractive index, coupled with high absorption, makes the reflectivity of a single layer extremely low, according to the Fresnel formula, just in the magnitude order of 10^{-4} under the incident condition. Therefore, ML coatings are the only useful optical components for normal incidence imaging in the EUV region[7−11]. Nowadays ML have been developed and used as optical key components in a variety of applications including synchrotron radiation (SR), EUV space exploration, plasma diagnostics, and EUV lithography[12−14].

Generally, the traditional periodic ML only worked with HR at a central wavelength. For special purposes, non-periodic MLs offer engineers great flexibility to achieve spectral performance in EUV and soft-X-ray region. For example, using a U/Y_2O_3 ML separated by Si/Al buffer layers, Allred *et al.*[15,16] achieved HR for He II emission line at 30.4 nm but anti-reflectivity (AR) for the ionosphere He I emission at 58.4 nm. Wang *et al.*[17,18] used a non-periodic $[SiC/Mg]_{Layer=60}$ ML structure for the design of a dual function mirror, where the calculated theoretical reflectivity at 10° incident angle were 54.1% and 0.1% at 30.4 and 58.4 nm, respectively. The reflectivity of He I (58.4 nm) was largely suppressed without significant loss in reflection for 30.4 nm. Hecquet *et al.*[19,20] proposed a new method to design and deposit two kinds of two channel EUV ML mirrors with enhanced spectral selectivity for the structure of a stack of two periodic MLs separated by a buffer layer. The first mirror reflected Fe IX-X line (17.1 nm) and Fe XVI line (33.5 nm) with attenuation of He II line (30.4 nm). The second mirror reflected Fe IX-X line (17.1 nm) and He II line (30.4 nm) with attenuation of Fe XV (28.4 nm) line and Fe XVI (33.5 nm). Zuccon *et al.*[21,22] successfully designed, deposited and characterized an innovative ML structure with HR at 28.4 nm coupled with a strong rejection ratio for adjacent spectral features at 30.4 nm. Depositing an optimized capping layer structure on top of the ML to adjust the electric field distribution of ML was effective to suppress noise wavelength of 30.4 nm.

In this study, we design a two-channel ML with HR at 19.5 nm and LR at 30.4 nm, by using genetic algorithm (GA) optimization method based on a stack structure of two periodic MLs and Optilayer software. Due to the high stability and fairly HR at the wavelength range from 12.5 to 30.0 nm, Mo/Si material combination is chosen for designing the MLs. The Mo/Si non-periodic ML is deposited by the ultrahigh vacuum direct current (DC) magnetron sputtering system. The layer structure is determined by measuring and fitting the grazing-incident X-ray diffraction (XRD) data, The reflectivity performance is measured by using a reflectometer at Hefei SR facility.

GA[17,23], inspired by biological selection and genetic evolution, was a powerful optimization method to design

various MLs. Due to merited function adjusted according to the actual situation, GA was applicable to single-objection and multi-target optimization. Optilayer software is a powerful tool to design the MLs and was also used. For GA as a global optimization was effective to ML with dramatic changes of film thickness, we used GA method to design the new two-channel ML. GA is limited by the parameters of population, iteration number and computing time, but not by initial model. The target of the two-channel ML designed for near-normal-incidence operation without roughness was maximum at 19.5 nm and minimum at 30.4 nm.

The two-channel ML was designed with a new structure[21] shown in Fig. 1. The structure was a stack of two periodic MLs with different layer number (N), gamma (d_{Si}/D). A single periodic ML only achieved HR or LR at a single wavelength or incident angle. To achieve duel function, the two-channel ML was a stack of 19.5-nm HR ML and 30.4-nm LR ML. The procedure was as follows.

We designed a periodic ML with HR at 19.5 nm for 13° incident angle. The value of population and iteration number of GA optimization parameter were 2000 and 150. The merited function (MF) was chosen as

$$\mathrm{MF}_1 = R_{H=19.5\ \mathrm{nm}}. \tag{1}$$

The optimizing reflectivity of 19.5 nm Mo/Si periodic ML was shown in Fig. 2. It can be seen that the reflectivity tends to be saturated with the increment of the number of layers, so the number of layers of 30 was chosen while designing HR ML. The black line in Fig. 2 was the reflectance performance curve of 19.5 nm $[\mathrm{Mo/Si}]_{N=30}$ ML. The reflectivity at 19.5 nm was 39.21% without suppression at 30.4 nm.

The key element is an optimized capping layer structure deposited on top of the periodic ML. Based on the parameter of $[\mathrm{Mo/Si}]_{N=30}$ ML remaining unchanged, we only optimized the top two capping layer to suppresses the reflectance at 30.4 nm. A new non-periodic ML with HR at 19.5 nm and LR at 30.4 nm was designed for 13° incident angle. The value of population and iteration number of GA optimization parameter were 2000 and 150. The MF was chosen as

$$\mathrm{MF}_2 = R_{H=19.5\ \mathrm{nm}} \ln(1/R_{L=30.4\ \mathrm{nm}}). \tag{2}$$

The optimizing results of two MLs were shown in Fig. 3 and Table 1. The optimizing two-channel ML preserved the performance reflectance at the target wavelength of 19.5 nm (37.08%) and at the same time suppressed the reflectance at 30.4 nm (from 1.06% to 9.59×10^{-4}) obviously.

After design and optimization, two-channel non-periodic Mo/Si ML were prepared on silicon substrates (20×30 (mm), σ <0.5 nm) by use of the ultrahigh vacuum DC magnetron sputtering system[24]. The base pressure reached 2×10^{-4} Pa before deposition. The working gas was Ar (purity 99.999%). The sputtering sources worked in a constant power mode. Compared with deposition rate curve calibration of traditional non-periodic MLs, the two channel ML method is simply to determine two periodic deposition rates. It greatly simplifies the fabrication process. The MLs were measured by grazing-incident XRD for determining individual layer thickness, interfacial roughness, and density of Mo and Si layer by fitting the measured data.

Two kind samples of periodic and two-channel MLs were deposited with design structure. The measured results were shown in Fig. 4. The wave trough of red line (two-channel ML) was different from the one of black (periodic ML) due to the top capping layers of two-channel ML. Because the curve mainly dependents on the periodic structure, the thickness of top capping

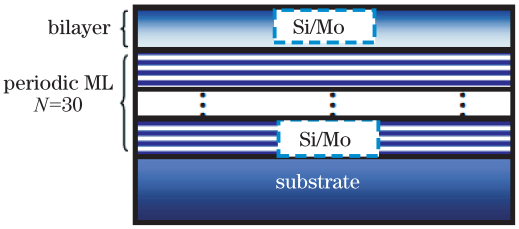

Fig. 1. Schematic design of two-channel ML.

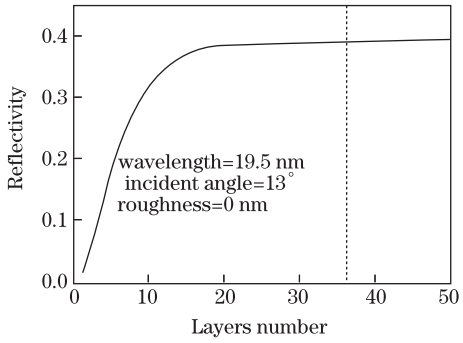

Fig. 2. Theoretical calculated reflectivity of the Mo/Si periodic ML.

Table 1. Two Channel $[\mathrm{Si/Mo}]_N$ ML (nm) with Roughness is 0 nm and Incident Angle is 13°

No.		N	Period d	$R_{19.5\ \mathrm{nm}}$	$R_{30.4\ \mathrm{nm}}$
Two-channel ML	Si	1	16.75	37.08%	2.17×10^{-7}
	Mo		1.98		
	Si	30	7.82		
	Mo		2.66		
Periodic ML	Si	30	7.82	39.21%	1.06%
	Mo		2.66		

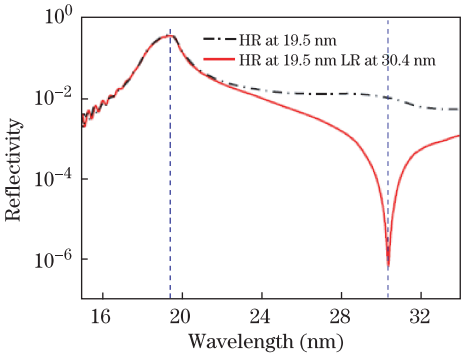

Fig. 3. (Color online) Theoretical calculated reflectance of the Mo/Si periodic and two-channel ML.

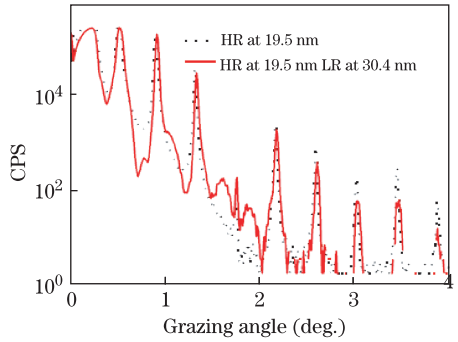

Fig. 4. (Color online) Grazing-incident XRD measured data of the Mo/Si periodic and two-channel ML.

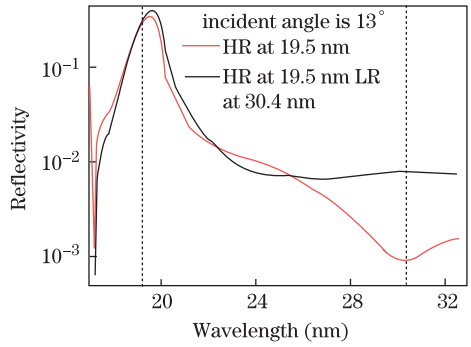

Fig. 5. (Color onlion) SR measured reflectivity of the Mo/Si periodic and two-channel ML.

Table 2. Two Channel [Si/Mo]$_N$ ML Measurement Results at 13° Incident Angle

Value		$R_{H=19.5\ \mathrm{nm}}$	$R_{L=30.4\ \mathrm{nm}}$
Two-channel ML	Theoretical	37.08%	2.17×10^{-7}
	Measured	33.31%	9.59×10^{-4}
Periodic ML	Theoretical	39.21%	1.06%
	Measured	37.77%	0.82%

bilayer cannot be determined from fitting the grazing-incident XRD directly. The thickness of top capping bilayer was ascertained by fitting the other periodic ML with the same top capping periodic structure. The thicknesses of periodic ML and two-channel ML were the same and satisfied the design value.

The reflectivities of the two-channel and periodic Mo/Si ML were measured with a reflectometer at the Spectral Radiation Standard and Metrology station on beamline U27 at the national synchrotron radiation laboratory (NSRL) in Hefei, China[25]. At the wavelength range from 17 to 25 nm, the samples were measured with 600 L/mm grating and Al filter. From 25 to 32 nm, the 600 L/mm grating and Mg filter was used. The measuring results were shown in Fig. 5 and Table 2.

At 19.5-nm wavelength, the experimental reflectivity reached 37.77% for the periodic ML and 33.31% for the two-channel ML. Besides, the reflectivity curve of the two-channel ML suppressed the reflectance at 30.4 nm (0.82%). The experimental results were closed to theoretical design value.

In conclusion, we design and fabricate a new two-channel ML, which reflects Fe XII line (19.5 nm) with attenuation of the He II line (30.4 nm). The two-channel ML and periodic ML reflecting 19.5 nm (contrast sample) fabricated using DC magnetron sputtering method are characterized by grazing-incident XRD and synchrotron reflectometer. The grazing-incident XRD data show that the prepared layer thickness is in line with the designed values. The measured reflectivity reaches 33.31% at 19.5 nm and 9.59×10^{-4} at 30.4 nm. Compared with the periodic ML with the same periodic number, the working wavelength and the incident angle, the two-channel ML suppresses the reflectivity at 30.4 nm from 0.82% to 9.59×10^{-4}. The two-channel ML is obtained with a stack of two periodic ML and will be applied to observe other emission lines in the EUV region, as well as the two-channel method will be used to space science research.

This work was supported by the National Natural Science Foundation of China under Grant No. 11027507.

References

1. J. P. Delaboudiniere, G. E. Artzner, J. Brunaud, A. H. Gabriel, J. F. Hochedez, and F. Millier, Sol. Phys. **162,** 291 (1995).
2. V. Slemzin, S. Kuzin, I. Zhitnik, J. P. Delaboudiniere, F. Auchere, A. Zhukov, R. Linden, O. Bugaenko, A. Ignat'ev, A. Mitrofanov, A. Pertsov, S. Oparin, A. Stepanov, and A. Afanas'ev, Sol. Sys. Res. **39,** 489 (2005)
3. A. K. Dupree, Astrophys. J. **178,** 527 (1996).
4. T. Yoshida and S. Tsuneta, Astrophys. J. **459,** 342 (1996).
5. M. F. Ravet, F. Bridou, X. Zhang-Song, A. Jerome, F. Delmotte, R. Mercier, M. Bougnet, P. Bouyries, and J. P. Delaboudiniere, Proc. SPIE **5250,** 99 (2004).
6. A. J. Corso, P. Zuppella, P. Nicolosi, D. L. Windt, E. Gullikson, and M. G. Pelizzo, Opt. Express **19,** 13963 (2011).
7. E. Meltchakov, C. Hecquet, M. Roulliay, S. D. Rossi, Y. Menesguen, A. Jérome, F. Bridou, F. Varniere, M. F. Ravet-Krill, and F. Delmottel, Appl. Phys. A **98,** 111 (2010).
8. D. L. Voronov, E. H. Anderson, R. Cambie, S. Cabrini, S. D. Dhuey, L. I. Goray, E. M. Gullikson, F. Salmassi, T. Warwick, V. V. Yashchuk, and H. A. Padmore, Opt. Express **19,** 6320 (2011).
9. E. Meltchakov, C. Hecquet, M. Roulliay, S. D. Rossi, Y. Menesguen, A. Jérome, F. Bridou, F. Varniere, M. F. Ravet-Krill, and F. Delmottel, Appl. Phys. A **98**, 111 (2010).
10. J. H. Underwood and T. W. Barbee, Appl. Opt. **20,** 3027 (1981).
11. A. Khandar and P. Dhez, Proc. SPIE **563,** 158 (1985).
12. B. W. Smith, J. J. Bloch, and D. R. Dupre, Proc. SPIE **1160,** 171 (1989).
13. N. M. Celgio, J. X-ray Sci. Technol. **1,** 7 (1989).
14. Z. Wang, F. Wang, Z. Zhang, H. Wang, W. Wu, S. Zhang, Y. Xu, Z. Gu, X. Cheng, C. Li, Y. Wu, B. Wang, S. Qin, and L. Chen, Opt. Prec. Eng. (in Chinese) **13,** 512 (2005).
15. D. D. Allred, R. S. Turley, and M. B. Squires, Proc. SPIE **3767,** 280 (1999).
16. S. Lunt, R. S. Turley, and D. D. Allred, J. X-ray Sci. Technol. **9,** 1 (2001).
17. Z. S. Wang, J. T. Zhu, R. Chen, J. Xu, F. L. Wang, Z. Zhang, J. Xu, W. J. Wu, L. Q. Liu, H. J. Zhang, D. Xu,

H. Jiang, L. Y. Chen, H. J. Zhou, T. L. Huo, M. Q. Cui, and Y. D. Zhao, Proc. SPIE **6984,** 698433 (2008).

18. Z. S. Wang, Proc. SPIE **7101,** 710110 (2008).
19. C. Hecquet, F. Delmotte, M. F. Ravet-Krill, S. Rossi, A. Jérome, F. Bridou, F. Varnière, E. Meltchakov, F. Auchère, A. Giglia, N. Mahne, and S. Nanaronne, Appl. Phys. **A95,** 401 (2009).
20. J. Gautier, F. Delmotte, and M. F. Ravet, Opt. Commun. **281,** 3032 (2008).
21. S. Zuccon, D. Garoli, M. G. Pelizzo, P. Nicolosi, S. Fineschi, and D. Windt, in *Proceedings of* 6*th International Conference on Space Optics* (2006).
22. M. Suman, M. G. Pelizzo, D. L. Windt, and P. Nicolosi, Appl. Opt. **48,** 5432 (2009).
23. M. Zhou and S. Sun, *Genetic Algorithms*: *Theory and Applications* (in Chinese) (National Defence Industry, Beijing, 2005).
24. J. T. Zhu, Z. S. Wang, Z. Zhang, and F. Wang, Appl. Opt. **47,** 310 (2008).
25. S. Xue and J. Shao, Opt. Prec. Eng. (in Chinese) **12,** 480 (2004).